

Grazing Incidence X-ray Diffraction of Merocyanine J-Aggregate Monolayers at the Air-Water Interface

Noritaka Kato, Kazuya Yuasa, Takeshi Araki, Yoshiaki Uesu,
Ichiro Hirosawa,* Masugu Sato,* Naoshi Ikeda,* and Ken-ichi Iimura**

Department of Physics, Waseda University, Tokyo 169-8555, Japan

Fax: +81-3-3202-4962, e-mail: n.k@waseda.jp

*Japan Synchrotron Radiation Institute, Hyogo 679-5197, Japan

**Department of Applied Chemistry, Utsunomiya University, Utsunomiya 321-8585, Japan

The visible absorption band of the merocyanine J-aggregates monolayer at the air-water interface (Langmuir (L) film) is blue-shifted and broadened after a multilayer formation by means of a Langmuir-Blodgett (LB) method. To discuss this spectral difference, a grazing incidence X-ray diffraction method was applied to the L and the LB films of the merocyanine J-aggregates. Since both in-plane molecular arrangements were almost the same, it was suggested that the interlayer dipole interactions made a change in the absorption spectrum of the J-aggregate L film.

Key words: Grazing incidence X-ray diffraction, J-aggregates, Langmuir film, Langmuir-Blodgett film

1. INTRODUCTION

J-aggregates [1] of organic dye molecules are characterized by a sharp, intense and red-shifted visible absorption band (J-band) compared to that of monomeric dye molecules. They have ordered molecular arrangements, and the electric dipole and the transition dipole interactions among the molecules allow them to form the J-band [2].

The J-aggregates have been used for spectral sensitizers of silver halides in conventional photography [3]. For the last decades, their potential technological application has been shown for opto-electronic devices such as solar cells, nonlinear optical devices, and optical memories [4-6]. Furthermore, in the cell biology, they have been used as fluorescent probes for detecting cellular apoptosis [7, 8]. These technological importances of J-aggregates have stimulated the fundamental researches on their inherent optical properties [1,9], and extensive studies have been made to relate the J-band wavelength to the structure of the J-aggregate [10,11].

So far, we have investigated the J-aggregates of merocyanine dye (MD) molecules* formed at the air-water interface (Langmuir film) [12 - 14]. The molecular structure is shown in Fig. 1. Morphologies of their Langmuir (L) and Langmuir-Blodgett (LB) films were clarified by nonlinear optical microscopy and atomic force microscope, respectively. It was found that MD J-aggregates were 2 dimensional (2D) crystallites of MD molecules with the size of several hundreds nm to several tens μm . However, in the case of MD J-aggregates, there is an issue that the wavelength and the width of the J-band are not the same in the L and the LB films. To clarify this difference between the L and LB films, we performed X-ray diffraction studies for both films and compared their 2D lattice structure. For

observing the diffraction pattern from the in-plane structure of the films, a grazing incidence X-ray diffraction (GIXD) method was applied. Specifically, a synchrotron radiation was used for the L film, because of an extremely low diffraction rate of a single molecular layer, i.e., the absolute number of organic molecules, which contribute to the X-ray scattering, is very small.

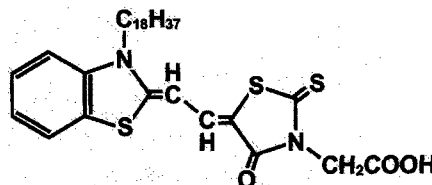


Fig. 1 Molecular structure of MD molecule.

2. EXPERIMENTAL DETAILS

2.1 Materials

MD molecule was purchased from Hayashibara Biochemical Laboratory, Inc. and 1 mmol/L chloroform solution of MD molecule was prepared for a spreading solution. Chloroform, MgCl_2 , CdCl_2 and NaHCO_3 were purchased from Kanto Kagaku. Pure water was prepared in a Milli-Q system and was used for aqueous subphase solutions. MgCl_2 and CdCl_2 were to supply the counter-ions of MD molecules, and the salt concentration of the subphase was 0.5 mmol/L, and NaHCO_3 was added to keep the pH value of the subphase ca. 6.8.

2.2 L film

The subphase consisting of MgCl_2 was used to obtain the MD J-aggregate, whose J-band is at 618 nm. The MD spreading solution was dripped on the subphase as a trough, which was home-built for GIXD measurements, until the monolayer covers the whole surface of the subphase, and the surface pressure was ca. 5 mN/m or

* 3-carboxymethyl-5-[2-(3-octadecyl-2(3H)-benzo-thiazolylidene)-ethylidene]-2-thioxo-4-thiazolidinone

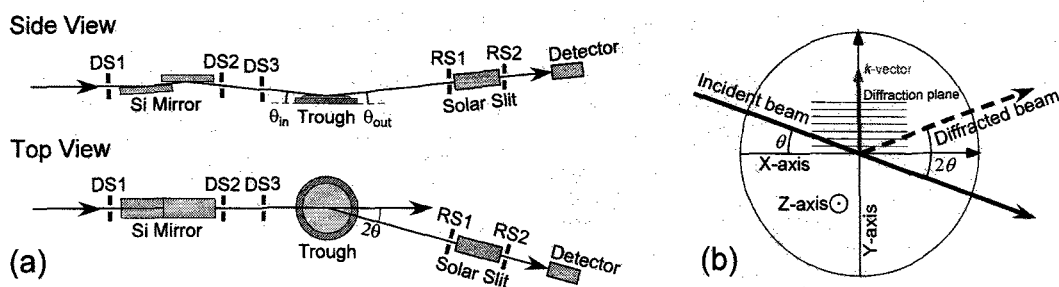


Fig. 1 Optical setups of the GIXD method for the L film (a) and the LB film (b).

less. Here, we note that, after being spread on the subphase, MD molecules form J-aggregates within a second even at fairly low surface pressure (< 5 mN/m), i.e., the MD monolayer is classified in a condensed monolayer. The temperature of the subphase was kept 17 ± 0.25 °C for all measurements.

A synchrotron radiation source of BL46UX at SPring-8 (Hyogo, Japan) was used for the GIXD measurements on the L film. The photon flux of the beam was the order of 10^{12} photons/sec in 0.1% beam-width. Optical setup is illustrated in Fig. 1(a). The X-ray energy was 12 keV ($\lambda = 0.103$ nm) and the cross-section of the beam was collimated into 1mm width and 0.1mm height by the divergence slits (DS1 and DS2). The incident angle θ_{in} was adjusted by the two Si-mirrors at 0.08° , which is below the critical angle of the total reflection for water. The trough was mounted on the eight-axes diffractometer, and a scintillation counter was used for the detection. The take-off angle θ_{out} was also set at 0.08° . Because the J-aggregate crystallites were oriented in a random direction on the subphase, the 2θ scan enabled us to observe the 2D powder diffraction of the L film. By using the receiving slits (RS1 and RS2) and the solar slit, the resolution of 2θ and θ_{out} was set to be 0.2° and 1° , respectively. The signal was accumulated for more than 30 sec on each scan steps.

2.3 LB film

Because the L film on the subphase containing only $MgCl_2$ cannot be deposited in a multilayered LB film, the mixture of 0.1 mmol/L of $CdCl_2$ and 0.4 mmol/L of $MgCl_2$ was used as a subphase. On this binary counter-ion subphase, the J-band locates at the same wavelength as that of the MD J-aggregates formed on the single counter-ion subphase of $MgCl_2$ when the subphase temperature is below 23 °C [13]. 20 layers of the L film on this binary counter-ion subphase at 15 °C were deposited on a hydrophobized glass slide by the LB method (vertical dipping method). The surface pressure on the deposition is kept at 20 mN/m. The dipping direction is defined as the x-axis, and the normal direction of the LB film as the z-axis for sample coordinates. The GIXD measurements on this LB film were performed by ATX-G (Rigaku, Ltd., Co.) equipped with a high power X-ray source of a rotating anode generator (100 Mcps at the sample). The incident X-ray beam (Cu $K\alpha$, $\lambda = 0.154$ nm) was collimated by the solar and the divergence slits into 10 mm width and 0.1 mm height. The incident angle was set at an angle of 0.2° to

the sample surface. The resolution of 0.4° in 2θ was obtained using the solar slit equipped before the scintillation counter. Fig. 1(b) indicates the diffraction geometry. The X-, Y- and Z-axes are the coordinates of the diffractometer. The sample was mounted as $z // Z$ and $x // X$, and the θ - 2θ scan was carried out to obtain the GIXD pattern. On this scan, the scattering vector k was always parallel to the x-axis of sample at any θ angle.

3. RESULTS

3.1 Visible Absorption Spectra of the L and the LB Films

The visible absorption spectra of the L and the LB films were shown in Fig. 2. The L film of monomeric MD molecules on the subphase, whose pH value was lowered by adding aqueous HCl, exhibited a similar absorption band to that of the chloroform solution of MD molecules. Besides the monomer band around 525 nm, the L film on the $MgCl_2$ subphase show the clear J-band at 618 nm. Although the L film on the present binary counter-ion subphase at 15 °C also exhibited the J-band at 618 nm [13], the absorption spectrum is not the same when it was assembled into the LB film. The band was broadened in the range of 613 to 605 nm, and the apparent band center became ca. 610 nm. Another

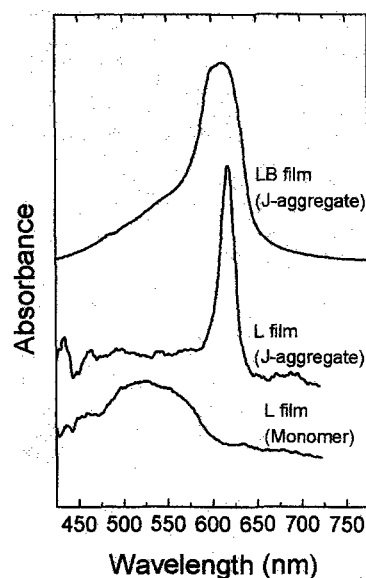


Fig. 2 Visible absorption spectra of the L and LB films of MD molecules.

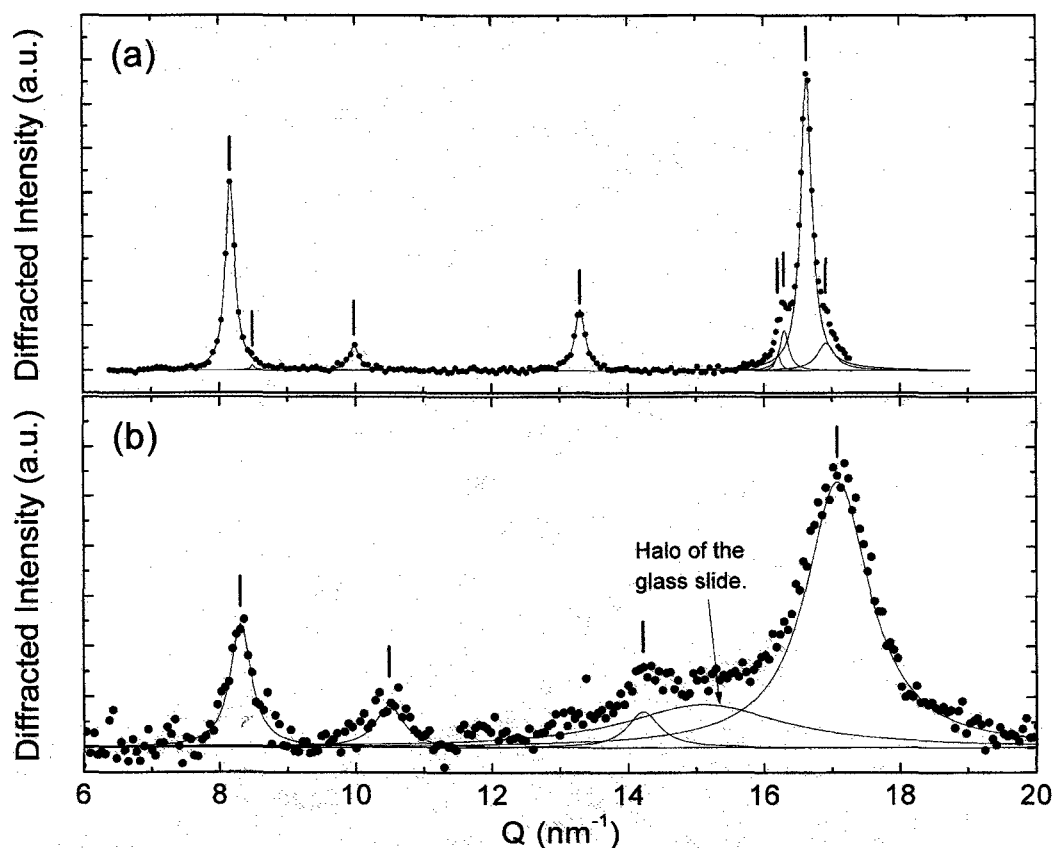


Fig. 3 GIXD patterns of L film (a) and LB film (b). The curves and the bars indicate the Lorentz functions fitted to each peaks and those peak positions. $Q = 4\pi\sin\theta/\lambda$ with the X-ray wavelength of λ and the diffraction angle 2θ .

feature of the band of the LB film was that the band exhibited a long tail toward the shorter wavelength side.

3.2 GIXD Measurements on the L Film

The observed GIXD pattern was fitted by polynomial and Lorentz functions for the background and diffraction peaks, respectively. The pattern after extraction of the background and correction of the Lorentz factor is shown in Fig. 3(a) together with the Lorentz functions. Four clear Bragg's peaks with four weak peaks were observed. To obtain this whole pattern, the 2θ scan was carried out four times and the four patterns were connected. In each scans, the L film was freshly prepared on the subphase having the same content and temperature.

3.3 GIXD Measurements on the LB Film

The observed GIXD pattern was fitted by polynomial and Lorentz functions for the background and diffraction peaks, respectively. The pattern after extraction of the background is shown in Fig. 3(b) together with the Lorentz functions. The θ - 2θ scan was performed on one sample without any termination. Four characteristic peaks at similar Q values to those of the L film were observed together with the very broad peak around $Q = 15 \text{ nm}^{-1}$. This broad peak is attributed to a halo from the glass slide. The widths of the four characteristic peaks observed on the LB film are broader than those of the L

film. This suggests that the size of the J-aggregate crystallites (grains) is smaller in the LB film than the L film. However, we have to take into account the difference of the directivity of the incidence and the resolution of the detection between two diffractometers.

4. DISCUSSION

4.1 Lattice structure

When we consider the base centered lattice shown in Fig. 4 having the lattice parameters shown in Table 1 (L

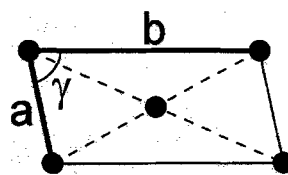


Fig. 4 2D lattice structure

Table 1 Lattice parameters and area per molecule of the L and the LB films

	L film	LB film
a (nm)	0.771	0.742
b (nm)	1.572	1.518
γ (rad)	1.365	1.375
Area/molecule (nm ²)	0.593	0.552

Table 2 Comparison of the observed and calculated diffraction positions of L and LB films

Miller Indices ^a (<i>h l</i>)	L film		LB film	
	Observed Q (nm ⁻¹)	Calculated Q (nm ⁻¹)	Observed Q (nm ⁻¹)	Calculated Q (nm ⁻¹)
(0 2)	8.167	8.164	8.305	8.440
(1 1)	8.493	8.493	---- ^b	8.845
($\bar{1}$ 1)	9.987	9.997	10.487	10.323
(1 3)	13.306	13.327	14.219	13.870
($\bar{1}$ 3)	16.210	16.157	---- ^b	16.654
(0 4)	16.305	16.328	---- ^b	16.880
(2 0)	16.636	16.657	17.084	17.273
(2 2)	16.917	16.985	---- ^b	17.690

^a Peaks of other indices are not observed due to extinction rule of the base-centered lattice shown in Fig. 4.

^b The peak was not observed.

film), the all peaks observed on the L film (Fig. 3(a)) are assignable. The Miller indices of each peak are summarized in Table 2 (L film), and good agreements between the observed and calculated peak positions clearly show that the lattice structure and its parameters (Fig. 4 and Table 1) are correct.

In the case of LB film (Fig. 3(b)), only the four peaks are visible and the other peaks are difficult to be extracted from the diffraction pattern. However, there is similarity in the relative intensities and positions of these four peaks between the LB and L film. (Fig. 3) Therefore, we assumed that the unit cell (Fig. 4) of the L film is the same as that of the LB film. This assumption is also supported by the fact that the J-band before deposition is the same as that of the L film observed in Fig. 3(a). The observed four peaks on the LB film are assigned into the same Miller indices as the corresponding peaks of the L film (Table 2 (LB film)), and the lattice parameters are then determined based on this peak assignment. The determined parameters are listed in Table 1 (LB film), and the observed and calculated peak positions are summarized in Table 2 (LB film). We cannot obtain the agreements as good as the case of the L film. However, when the larger peak width and lower signal to noise than the case of the L film are taken into account, the deviations between the observed and calculated peak positions are reasonably acceptable.

In Fig. 5, the determined lattices of the L and the LB films are compared in a same scale. Contraction of the lattice in the LB film is clearly shown in Fig. 5, as the Q values of the four peaks of the LB film are larger than those of the L film, and there is almost no distortion, i.e., isotropic contraction. The area of 7 % on the unit cell of the L film was lost in the LB film. Except this contraction, it is clarified that the average lattice structure was maintained during the deposition of the multilayer by the LB method.

The 2D lattice contraction in the LB film could be attributed to the surface compression of the L film on the LB deposition and/or the water evaporation from the film after deposition. The former contribution can be related to a surface pressure-area (π -A) isotherm. According to the π -A isotherm of the L film on the MgCl₂ subphase at ca. 20 °C, the molecular occupation area at 5 mN/m is 0.61 nm² and at 20 mN/m, where the deposition was performed on the preset LB film, is 0.57 nm². Although the absolute values of area/molecule in

the lattices shown in Table 1 are 4 % larger than those obtained by π -A isotherm, the difference in molecular occupation area between 5 and 20 mN/m corresponds well to that in the lattice structure, i.e., the area at 20 mN/m is 7 % smaller than that at 5 mN/m. However, we should mention that the π -A isotherm is affected by the compressibility among the MD J-aggregate domains (grains) and not always the response from the MD J-aggregate itself. On the other hand, the X-ray diffraction reflects the molecular arrangement inside the J-aggregate domain.

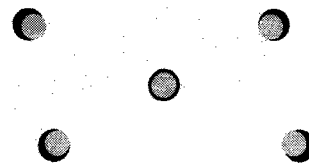


Fig. 5 Comparison of the lattices. Black large points and gray small points indicate the lattice of the L and the LB films, respectively. The point at the base-center of both lattices is plotted at the same position.

4.2 Difference of J-Band between the L and LB Films.

When the 2D lattice is isotropically contracted, the dipole interactions in the layer are obviously enhanced as a result of a decrease in intermolecular distances. The enhancement of the dipole interactions then results in a further red-shift of the absorption band. However, the J-band was blue-shifted and broadened after deposition (Fig. 1), even though the lattice structure was maintained well. This suggests that the dipole interactions among the layers have to be considered in the case of the LB film. The bilayer interval of the LB film is 3.3 nm, and the dipole interactions reaches up to in the order of 100 nm. Thus, the 3 dimensional dipole interactions are essentially required for discussing the J-band of the LB film. Furthermore, the broadening of the diffraction peak observed on the LB film implies that the size of the crystallites became smaller after the deposition, and this contributes to the blue-shift of the J-band.

5. CONCLUSIONS

The GIXD patterns of the L and the multilayered LB

films of MD molecules were observed. Specifically, in the case of the L film, the synchrotron radiation (SPRING-8) was used. According to the comparison between the determined 2D lattice structures of the films, it was clarified that the molecular arrangement in the L film is maintained well after the deposition on the glass slide by the LB method except the 2D isotropic contraction of 7 % in the LB film. This 2D contraction is due to the surface compression of the L film during the deposition of LB film.

Both samples had the same J-band on the subphase, but not in the multilayered LB film. Because the average molecular arrangements are basically the same in both films, this spectral change in the LB film is attributed to the interlayer interaction of the electric and transition dipole moments among the MD molecules in the LB film. Furthermore, the broadening of the diffraction peaks of LB film suggests that the size of the J-aggregates became smaller. This size effect should also affect the spectral change of the J-band.

6. ACKNOWLEDGMENTS

The synchrotron radiation experiments were performed at the SPRING-8 with the approval of the Japan Synchrotron Research Institute (JASRI) (Proposal No. 2002B0706-ND1-np and 2004A0247-ND1d-np). Present work was supported by the SANEYOSHI Scholarship Foundation (No. 1610) and the Grant-in-Aid for The 21st COE Program (Physics of Systems with Self-Organization Composed of Multi-Elements) at Waseda University from the Ministry of Education, Culture, Sports, Science and Technology, Japan.

References

- [1] T. Kobayashi (Ed.), "J-Aggregates", World Scientific, Singapore (1996).
- [2] A. S. Davydov, "Theory of Molecular Excitons", McGraw-Hill, New York (1962).
- [3] T. Tani, *J. Disp. Sci. Technol.*, **25**, 375 (2004).
- [4] K. Sayama, S. Tsukagoshi, K. Hara, Y. Ohga, A. Shinpou, Y. Abe, S. Suga, and H. Arakawa, *J. Chem. Phys. B*, **106**, 1363 (2002).
- [5] M. Furuki, M. Tian, Y. Sato, L. S. Pu, S. Tatsuura, and O. Wada, *Appl. Phys. Lett.*, **77** 472 (2000).
- [6] E. Ando, J. Miyazaki, K. Morimoto, H. Nakahara, and K. Fukuda, *Thin Solid Films*, **133** 21 (1985).
- [7] S. Smiley, M. Reers, C. Mottola-Hartshorn, M. Lin, A. Chen, T. W. Smith, G. D. Steele Jr., and L. B. Chen, *Proc. Natl. Acad. Sci. U.S.A.*, **88**, 3671 (1991).
- [8] L. Liu, J. R. Trimarchi, and D. L. Keefe, *Biol. Reprod.*, **62**, 1745 (2000).
- [9] E. G. McRae and M. Kasha, "Physical Processes in Radiation Biology", edited by L. Augenstein, R. Mason, and B. Rosenberg, Academic Press, New York (1964), Chap. 3, pp. 23-42.
- [10] V. Czikkely, H. D. Forsterling, and H. Kuhn, *Chem. Phys. Lett.*, **6**, 207 (1970).
- [11] K. Ikegami, *J. Chem. Phys.*, **121**, 2337 (2004).
- [12] N. Kato, K. Saito, H. Aida, and Y. Uesu, *Chem. Phys. Lett.*, **312**, 115 (1999).
- [13] N. Kato, K. Saito, and Y. Uesu, *Chem. Phys. Lett.*, **326**, 395 (2000).
- [14] N. Kato, K. Saito, T. Serata, H. Aida, and Y. Uesu, "Ferroelectrics Vol. 2", edited by V. Stefan, The Stefan University Press Series on Frontiers in Science and Technology, La Jolla, CA (2002), pp81-110.

(Received December 23, 2004; Accepted January 31, 2005)